

Characterization and Doping Effect of Cu-Doped ZnO Films

Khin Khin Kyaw¹ and Hla Toe²

1. Department of Physics, University of Yangon, Kamayut 11041, Myanmar

2. Department of Physics, Panglong University, Panlong 06114, Myanmar

Abstract: Cu (copper)-doped ZnO (zinc oxide) was synthesized using $\text{Cu}(\text{NO}_3)_2 \cdot 3\text{H}_2\text{O}$ (copper (II) nitrate) and $\text{Zn}(\text{NO}_3)_2 \cdot 6\text{H}_2\text{O}$ (zinc nitrate) by chemical co-precipitation method. The weight percentages of dopant in solution were Cu (2, 3, and 5 wt %). Cu-doped ZnO thin films were prepared on p-Si (100) substrate by screen printing method. Cu-doped ZnO/Si films were annealed at different temperatures from 300 to 700 °C. In this study, Cu-doped ZnO structures were prepared by a simple precipitation technique, and characterized by various techniques such as XRD (X-ray diffraction) and SEM (scanning electron microscope). The electrical properties of Cu-doped ZnO/Si were measured. It has found that Cu-doped ZnO/Si films can be used as optoelectronic devices.

Key words: Copper doped zinc oxide, silicon, optoelectronic device, co-precipitation method.

1. Introduction

ZnO (zinc oxide) is an inexpensive, n-types semiconductor with a wide band gap having optical transparency in the visible range. It crystallizes in a hexagonal wurtzite structure with the following lattice parameters $c = 5.205 \text{ \AA}$, $a = 3.249 \text{ \AA}$ [1]. The n-type semiconductor behavior is due to the ionization of excess zinc atoms in interstitial positions and the oxygen vacancies. Surface defects play an important role in the photocatalytic activities of metal oxides as they increase the number of the active sites [2]. For this reason it is interesting to study the effect of ZnO doped by transition metals on its photocatalytic properties. Data are reported in the current literature about the influence of copper (Cu) dopant in ZnO powder and thin films on the photocatalytic behavior. Various techniques for preparation of ZnO have been applied: sol-gel method, the co-precipitation method etc. [3].

In this research work, the crystalline structure of the as-prepared Cu-ZnO films was characterized by XRD (X-ray diffraction). The surface microstructure was

obtained by SEM (scanning electron microscope). The UV (ultraviolet)-visible absorption of the samples was recorded using UV-Vis spectrometer in the wavelength range of 190-1,100 nm. Cu-ZnO/Si thin films were done by co-precipitation method and screen printing method [4]. We present the temperature dependent characterization and photovoltaic property of the samples to investigate the mechanism of photovoltaic effect. *I-V* (current-voltage) measurements are carried out to investigate the electrical properties of Cu-ZnO/Si heterojunction. For application in optoelectronic devices, the optimum film diffusion temperature should be chosen for the best devices performance.

2. Experimental Details

2.1 Synthesis of Undoped ZnO and Cu-Doped ZnO

The synthesis of undoped and Cu-doped ZnO samples has been prepared by co-precipitation method. Pure $\text{Zn}(\text{NO}_3)_2 \cdot 6\text{H}_2\text{O}$ (zinc nitrate) of analytical grade, $\text{Cu}(\text{NO}_3)_2 \cdot 3\text{H}_2\text{O}$ (copper II nitrate) of the various ratios (2, 3 and 5 wt %), ammonia and D/I (distill water) were used as reagent materials. In a typical experiment, $\text{Zn}(\text{NO}_3)_2$ and $\text{Cu}(\text{NO}_3)_2$ were dissolved

Corresponding author: Hla Toe, PhD, professor, research field: physics.

D/I water. Ammonia was added to solvent (drop by drop). The solvent were stirring on hot plate stirring. After 2 hr later, the white precipitation was deposited on the bottom of the flask. The solvent stirring process was shown for precipitation process in Fig. 1. The precipitate samples were centrifuged shown in Fig. 2a. The white solid was collected and washed several times with D/I, ethanol and dried in air with filter paper shown in Fig. 2b. After heat treated process Cu-doped ZnO powder was achieved shown in Figs. 3a and 3b. Slices of cleaned p-typed Si(100) were used as substrates for Cu-doped ZnO deposited on Si film. After the synthesis process, the Si (silicon) substrates were sequentially cleaned with an acetone, D/I water and HCl into the beaker and Si wafer dipped in the solution for 30 min. Cleaning work was shown in Fig. 4b. Etching solvent was used to remove organic contaminants and grease. After this step, substrates were rinsed with deionized water for 30 min. The final samples were heated for 3 h at 100°C and calcinated at 450°C for 1 h in furnace, this process is shown in Fig. 5b.

In this work, the best ratio of Cu-doped ZnO powder was placed into the beaker and mixed with 2-methoxyethanol (1 mL) and PPG (propylene glycol) and stirred homogeneously for 2 h. After that Cu-doped ZnO solvent was obtained to use for deposition on Si substrate. This process was shown in Fig. 4a. The Cu-doped ZnO solvent was deposited on clean Si substrate by screen printing method; it was shown in Fig. 5a. Then, finally the Cu-doped ZnO deposited on Si samples was placed into the furnace



Fig. 1 Stirring the solvent.



Fig. 2 (a) Centrifuge; (b) dried in air.



Fig. 3 (a) Pure ZnO powder; (b) Cu-doped ZnO.



Fig. 4 (a) Cu-ZnO solvent; (b) Si cleaning.



Fig. 5 (a) Screen printing process; (b) thermal diffusion process.



Fig. 6 Cu-ZnO/Si film 600 °C.

and annealed to samples at different temperatures from 300 to 700 °C for 30 min to each sample. Fig. 6 shows Cu-doped ZnO deposited on Si film at deposition temperature 600 °C. Experimental procedure of this research was clearly step by step shown in Fig. 7.

The samples were characterized by XRD using multiflex-2 kW type X-ray diffractometer with Cu-K α radiation. The particle morphologies of the ZnO powder and Cu-ZnO powder were observed by SEM. *I-V* characteristic of each sample was measured by LUX meter, Fluke-45 dual display multimeter and other supporting equipments.

2.2 Structural Properties of ZnO and Cu-ZnO/Si Device by XRD

The XRD spectra show the syntheses ZnO and Cu-ZnO were presented. The characterization of

Cu-ZnO/Si with respect to phase identification, crystal structure was determined by XRD with Cu-K α radiation. The XRD analysis of synthesized ZnO and Cu-doped ZnO deposited on Si at 600 °C was shown in Figs. 8 and 9 respectively. The XRD analysis of Cu-doped ZnO deposited on Si samples at different deposition temperatures was shown in Fig. 10. The crystallite size is calculated from peak broadening using Debye-Scherer formula ($D_{hkl} = \frac{0.899\lambda}{B \cos\theta}$). The average crystallite size of all samples was shown in Tables 1 and 2. XRD peaks (101) plane was shifted slightly depending on the deposition temperature. Fig. 8 shows the ZnO, similar to (Joint Committee on Powder Diffraction Standards) card No. 80-0075, formed in crystalline state. The crystallite size is calculated from dominant peak broadening of (101) plane.

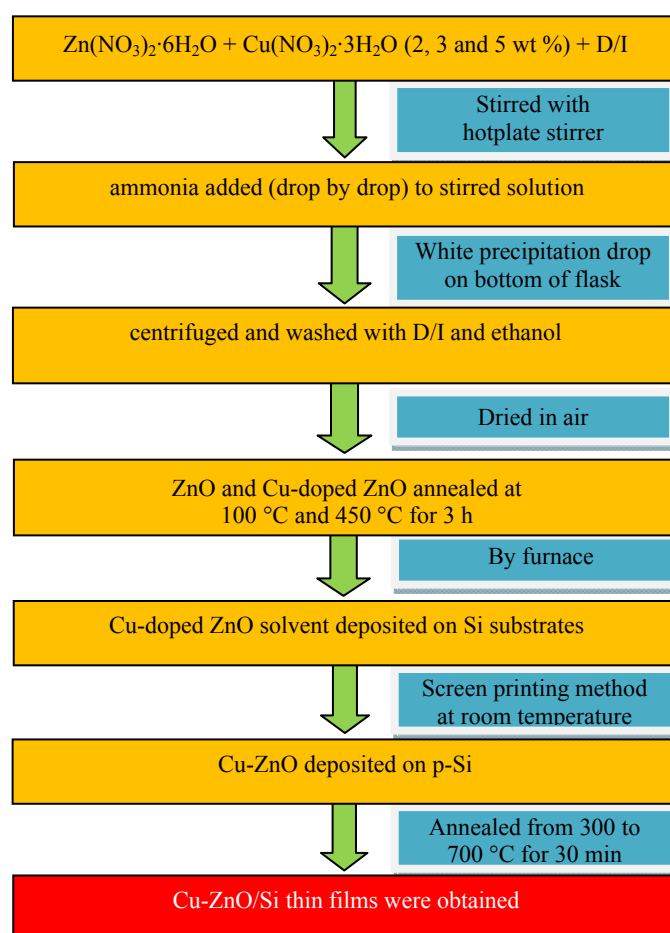


Fig. 7 Block diagram of synthesis of ZnO and Cu-doped ZnO/Si thin films.

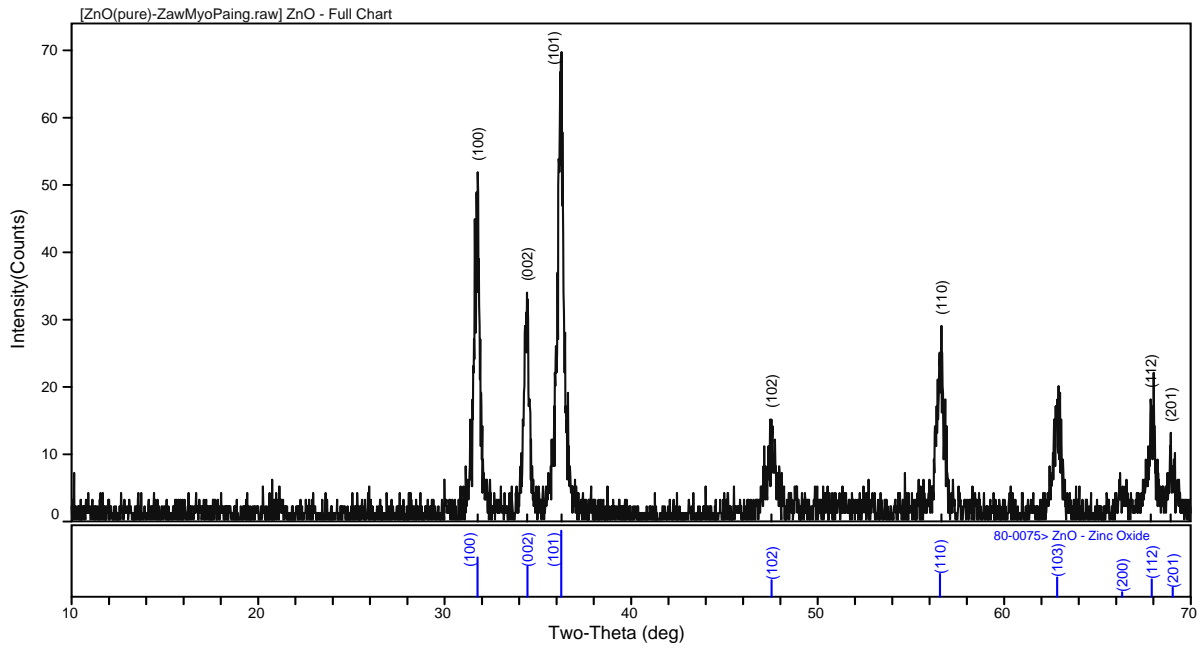


Fig. 8 The XRD analysis of synthesis of ZnO powder.

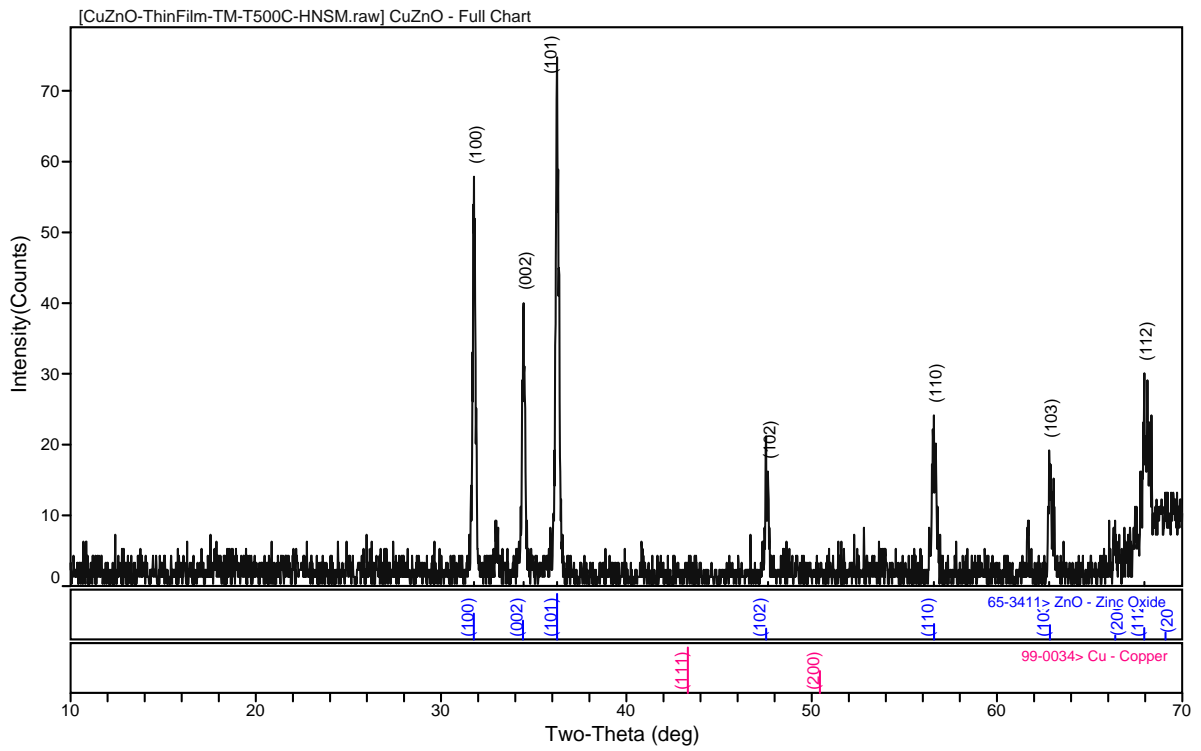


Fig. 9 The XRD of Cu-ZnO/Si thin film at 600 °C.

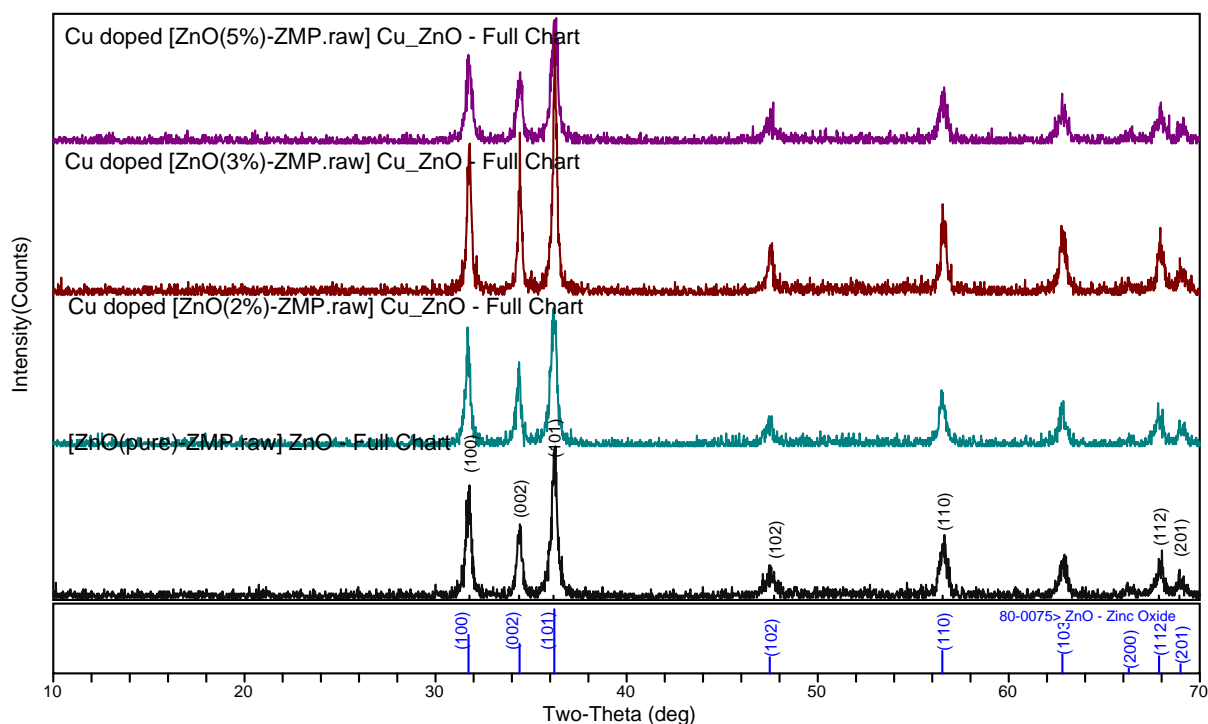


Fig. 10 Comparison of the XRD diffraction analysis of undoped and doped powder.

Table 1 Crystallite size calculation of undoped ZnO powder and Cu-doped ZnO powder.

Samples (different weight ratios)	2θ ($^{\circ}$)	hkl plane	FWHM	Lattice constant (a)	c/a	Crystal structure	Crystallite size (nm)
Undoped synthesis ZnO	36.278	(101)	0.340	3.2484	1.604	Hexagonal	24.55
Cu-ZnO synthesis powder ratio (2 wt %)	36.318	(101)	0.630	3.2511	1.602	Hexagonal	27.833
Cu-ZnO synthesis powder ratio (3 wt %)	36.259	(101)	0.227	3.2480	1.605	Hexagonal	36.783
Cu-ZnO synthesis powder ratio (5 wt %)	36.281	(101)	0.370	3.2538	1.601	Hexagonal	22.568

FWHM: full width at half maximum.

Table 2 Crystallite size calculation of Cu-doped ZnO/Si thin films (3 wt %).

Samples (different heat treatment temperature)	2θ ($^{\circ}$)	hkl	FWHM ($^{\circ}$)	Lattice constant (a)	c/a	Crystal structure	Crystallite size (nm)
300	36.279	(101)	0.202	3.2471	1.604	Hexagonal	41.34
400	36.319	(101)	0.208	3.2453	1.602	Hexagonal	40.15
500	36.226	(101)	0.172	3.2515	1.600	Hexagonal	48.54
600	36.259	(101)	0.198	3.2489	1.601	Hexagonal	42.17
700	36.260	(101)	0.181	3.2495	1.606	Hexagonal	46.13

Table 3 The energy band-gap of ZnO particles and Cu-doped ZnO particles.

Samples	λ (nm)	E_g (eV)
Pure ZnO	348	3.54
2 wt % Cu-doped ZnO	352	3.50
3 wt % Cu-doped ZnO	364	3.39
5 wt % Cu-doped ZnO	349	3.53

Analyses of XRD data for different peaks of ZnO corresponding to planes (100), (002), (101), (102), (110), (103), (200), (112) and (201) of hexagonal structure have been identified. Major diffraction peaks of ZnO exhibited a hexagonal structure with preferred grain orientations along (100), (002) and (101) plane, they were shown in Fig. 9. All of the peaks are well matched with the ZnO, which could be indexed as the hexagonal wurtzite structure of ZnO. You can see in comparison of Figs. 8 and 9.

The peaks of XRD spectrum correspond to those of synthesis ZnO and three different doping ratios of Cu-ZnO patterns from the JCPDS data having hexagonal wurtzite structure of the bulk with c/a ratio are 1.604 for undoped synthesis ZnO and 1.602, 1.605 and 1.601 for Cu-doped ZnO powder at different doping ratios (2, 3, 5 wt%). These data are mentioned in column 6 of Tables 1 and 2. The peaks of XRD spectrum correspond to those of the synthesis for Cu-doped ZnO/Si (3 wt %) patterns from the JCPDS data having hexagonal wurtzite structure of the bulk with c/a ratios of 1.604, 1.602, 1.600, 1.601, and 1.606 for different diffusion temperatures from 300 to 700 °C respectively. Comparison of these analysis data was shown in Table 3 column 6.

Three doping ratios of Cu-doped ZnO were 2θ shifted from undoped ZnO and (3 wt %) ratio was narrower than other ratio samples. They are clearly shown in column 2 of Tables 1 and 2. Degree of 2θ of (5 wt %) sample is nearly same as pure ZnO, it is denoted that Cu was nearly completely doped into ZnO. But some Cu ions are left by the (111) and (200) peak. You can see in Fig. 9. It's means that Cu ions were not completely doped into ZnO.

Crystal structure of Cu is cubic and ZnO is hexagonal. In the XRD result, all synthesized Cu-ZnO samples were hexagonal structure, so Cu was doped into ZnO because synthesized pure ZnO was also hexagonal structure.

2.3 SEM Analysis of Cu-Doped ZnO/Si Device

Typical SEM images for synthesis of ZnO and

Cu-ZnO were shown in Figs. 11a-11d. The size of ZnO grains is 0.25 μm. These SEM images show different morphology of surface grain size, which depend on different Cu doping ratios 2, 3, and 5 wt %. These images were shown in Figs. 11a-11d. These particles are uniform with size chain agglomeration and the average width and length of particles are 0.20 to 0.75 μm. According to our experimental result, the SEM images of doped samples, no significant change of their hexagonal structure morphology was observed. These data were shown in Table 3. Grain size depends on the doping ratio; increasing the ratio produces the larger grain size. SEM images of all samples clearly show hexagonal structure and it is coincidence of synthesis ZnO structure. Hexagonal structure patterns were clearly shown in Fig. 11c.

2.4 UV-Analysis of ZnO and Cu-ZnO

The measurement of the bandgap of materials is important in the semiconductor, nonmaterial and solar industries. The term "bandgap" refers to the energy difference between the top of the valence band to the bottom of the conduction band. The electrons are able to jump from one band to another. In order for an electron to jump from a valence band to a conduction band, it requires a specific minimum amount of energy for the transition, the bandgap energy [7].

The UV-vis DRS (diffuse reflectance spectra) of the synthesized ZnO and Cu-ZnO and UV spectra of Cu-doped ZnO particles are shown in Figs. 12 and 13 respectively. The spectrum reveals characteristic of absorption peak of ZnO at wavelength of 348 nm, which can be assigned to the intrinsic band-gap absorption of ZnO due to the electron transition from the valence band to the conduction band. The data get from UV graph as shown in Fig. 12. From the absorption peak, the optical energy band gap has been calculated using the formula:

$$E_g = hv = \frac{hc}{\lambda}$$

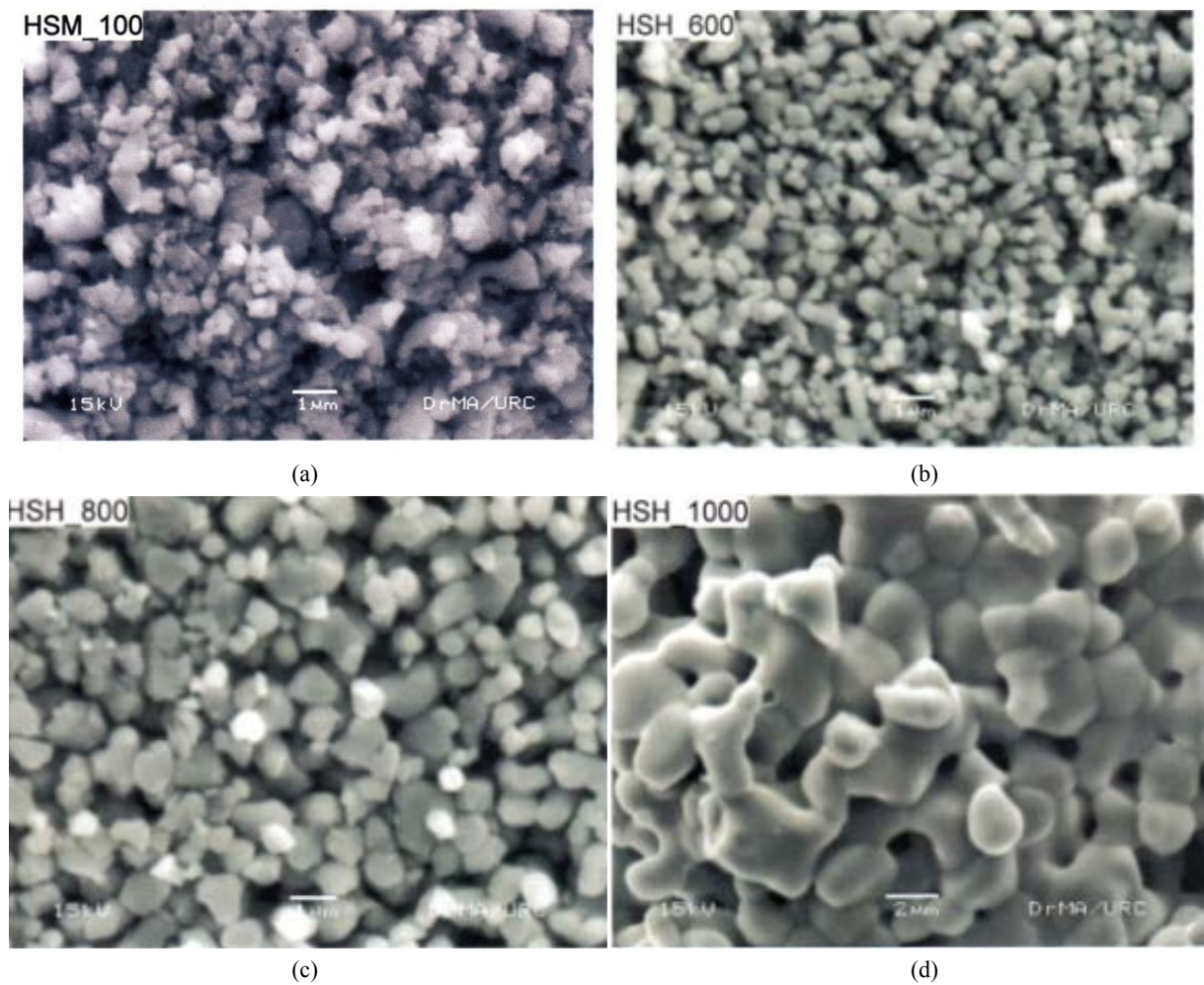


Fig. 11 (a) Synthesis of pure ZnO powder; (b) synthesis of Cu-ZnO powder (2%); (c) synthesis of Cu-ZnO powder (3%); (d) synthesis of Cu-ZnO powder (5%).

where h = plank's constant and E_g = energy band gap of the semiconducting particle in the optical spectra. The bandgap of Cu-doped ZnO was reduced more than undoped ZnO from 3.54 eV to 3.39 eV (3 wt % Cu-doped ZnO). The bandgap of undoped ZnO and Cu-doped ZnO could be determined by finding the wavelength turning edge of the UV-vis absorption peak. These data were shown in Figs. 12 and 13.

In this case, Cu^{2+} ions replaced Zn^{2+} ions and formed CuO in the ZnO. The CuO has a smaller bandgap (1.35 eV) as compared to ZnO (3.37 eV).

Thus, when the CuO was introduced into the ZnO lattice, the intrinsic bandgap of ZnO became narrower.

2.5 I-V Characteristic Measurement of Cu-ZnO/Si Thin Film

To determine the photovoltaic characterization of the Cu-ZnO/Si film, the I - V characteristics of illumination conditions was studied as shown in Fig. 14. Under the illumination condition, the reverse current strongly increases with illumination intensity of 1,000 LUX. I - V measurement of Cu-ZnO/Si device gives a maximum open circuit voltage V_{oc} and short-circuits current I_{sc} as shown in Tables 4 and 5.

$$\eta = \frac{P_{out}}{P_{in}} \Rightarrow \eta = \frac{P_{MAX}}{P_{in}}$$

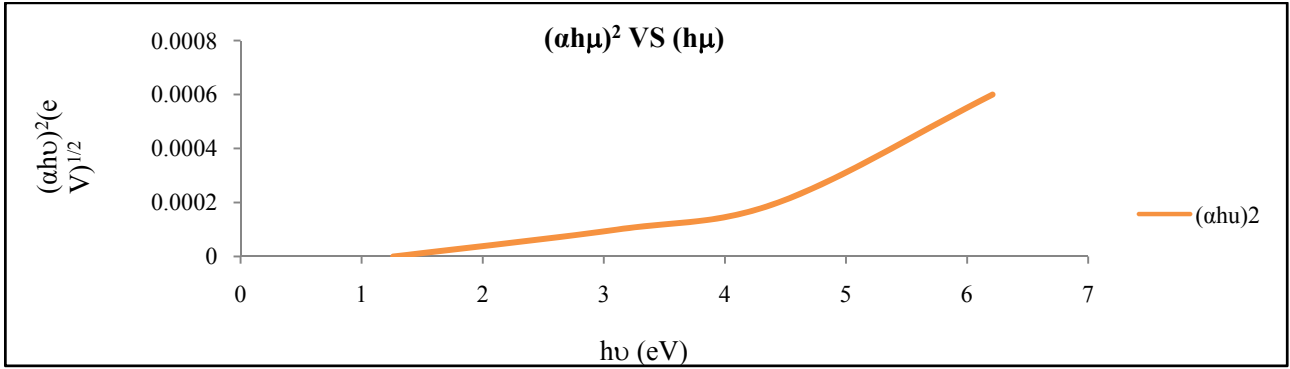


Fig. 12 The plot for band-gap energy (E_{bg}) of ZnO.

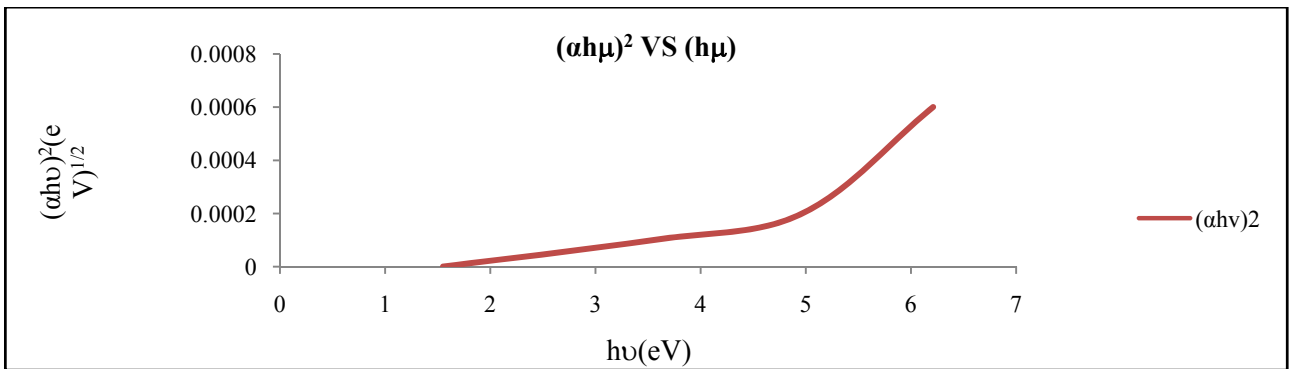


Fig. 13 The plot for band-gap energy (E_{bg}) of Cu-ZnO.

Table 4 The maximum current (I_m), maximum voltage (V_m), short circuit current (I_{sc}) and open circuit voltage (V_{oc}) of Cu-ZnO/Si film.

Annealed temperature	I_m	V_m	I_{sc}	V_{oc}
400 °C	3 μ A	30 mV	4.08 μ A	46.9 mV

Table 5 The conversion efficiency (η) and FF (fill factor) of Cu-ZnO/Si film.

Annealed temperature	η (%)	FF
400 °C	0.063	0.47

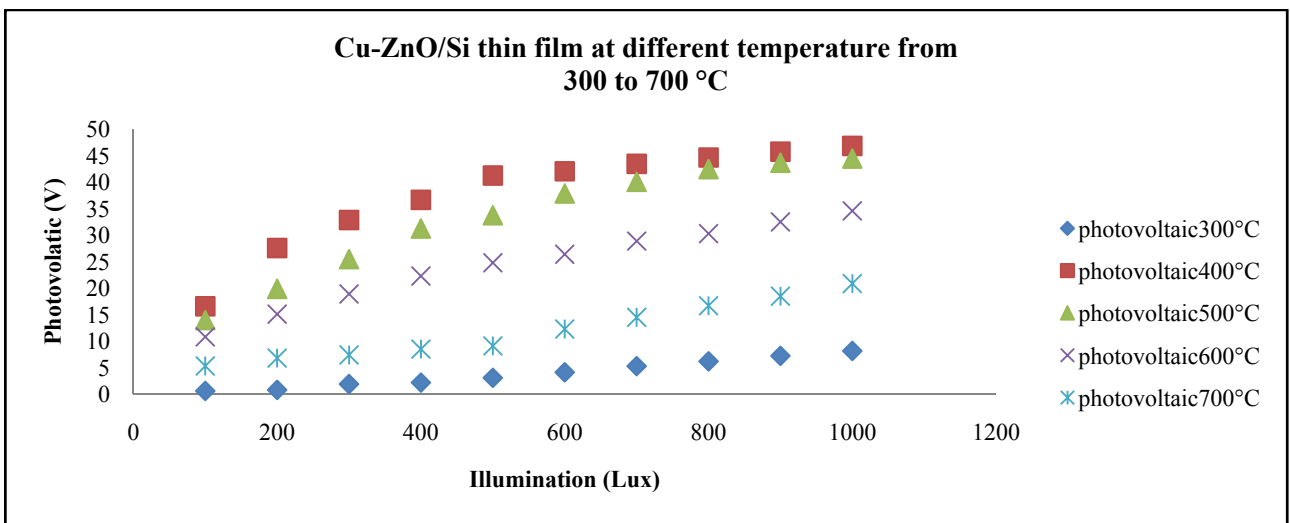


Fig. 14 Photovoltaic measurement of Cu-ZnO/Si film from 300 to 700 °C.

3. Discussion

Undoped ZnO and Cu-doped ZnO were successfully synthesized by Co-precipitation process for three different doping ratios (such as 2, 3, 5 wt %) and deposited on p-Si substrate by screen printing method. $\text{Zn}(\text{NO}_3)_2 \cdot 6\text{H}_2\text{O}$ was used as a starting materials and $\text{Cu}(\text{NO}_3)_2 \cdot 3\text{H}_2\text{O}$ is used as a dopant material in this research. The synthesized undoped ZnO and Cu-doped ZnO particles were found to be of single-crystal quality with hexagonal wurtzite structure. XRD measurements indicate that the synthesized ZnO crystals are in the hexagonal phase and dominant peaks are (100), (002) and (101). According to the SEM result, SEM images of Cu-doped ZnO show hexagonal particles with random form. Doping ratio (3 wt %) image shows clearly hexagonal structure but it has some holes, and can absorb moisture.

4. Conclusion

Cu-doped ZnO was synthesized by using co-precipitation method and Cu-doped ZnO was successfully deposited on p-Si substrate by screen printing method. The microstructure and morphological properties of the Cu-ZnO were investigated. The microstructure of Cu-doped ZnO was examined by XRD. The XRD patterns showed that the Cu-doped ZnO was of hexagonal structure and that the prepared film has the dominant peak of (101) preferred orientation. Crystallite size of Cu-doped ZnO thin film was changed on the different doping ratios (2, 3 and 5 wt %). In XRD analysis, the dominant peak of Cu-doped ZnO with doping ratio (3 wt %) is higher than other samples. Surface morphology of Cu-doped ZnO was checked by SEM. The SEM image showed that the Cu-doped ZnO exhibited a uniform surface morphology and hexagonal microstructure.

The microstructure of Cu-ZnO/Si films was checked by XRD. Crystallite size of Cu-ZnO/Si thin

film was changed at the different deposition temperatures. From the XRD result, the dominant peak (101) of diffusion temperature 400 °C is higher than other films. Smallest grain size of Cu-doped ZnO/Si film has diffusion temperature of 400 °C shown by the XRD pattern. From XRD results, the lattice constant c/a has been calculated for synthesis of pure ZnO and Cu-ZnO. With the doping concentration of 3 wt % the lattice constant a increases from 3.2480 Å to 3.2538 Å and c decreases from 5.2138 Å to 5.1892 Å. XRD results show Cu is successfully doped into ZnO in 3 wt % samples and in other samples were Cu was not completely doped into ZnO.

According to the UV-vis spectroscopy, bandgap energy of Cu-doped ZnO doping ratio 3 wt % was narrower than undoped ZnO and other doping ratios (2 and 5 wt %). It can cause better electron mobility than other doping ratios. Bandgap energy of Cu-doped ZnO depends on Cu concentration. According to the I - V characteristic measurement results Cu-doped ZnO/Si device shows solar cell behavior and it can be used for solar cell materials.

Acknowledgements

Authors deeply thank Professor Dr. Pho Kaung, Rector of University of Yangon for suggestion of this research work. We would like to thank Professor Dr. Khin Khin Win, Head of Department of Physics, University of Yangon, for valuable advices on our research.

References

- [1] Bahsi, Z., and Oral, A. 2007. "Effect of Mn and Cu Doping on the Microstructures and Optical Properties of Sol-Gel Derived ZnO Thin Films." *Optical Materials* 29 (6): 672-8.
- [2] Ullah, R., and Dutta, J. 2008. "Photocatalytic Degradation of Organic Dyes with Manganese-Doped ZnO Nanoparticles." *Journal of Hazardous Materials* 156 (1-3): 194-200.
- [3] Fu, M., Li, Y., Wu, S., Lu, P., Liu, J., and Dong, F. 2011. "Sol-Gel Preparation and Enhanced Photocatalytic Performance of Cu Doped ZnO Nanoparticles." *Applied Surface Science* 258 (4): 1587-91.

- [4] Rekha, K., Nirmala, M., Nair, M., and Anukalini, A. 2010. "Structural, Optical, Photocatalytic and Antibacterial Activity of Zinc Oxide and Manganese Doped Zinc Oxide Nanoparticles." *Physica B* 405 (15): 3180-5.
- [5] Xu, C., Cao, L., Su, G., Liu, W., Liu, H., Yu, Y., and Qu, X. 2010. "Preparation of ZnO/Cu₂O Compound Photocatalyst and Application in Treating Organic Dyes." *Journal of Hazardous Materials* 176 (1-3): 807-13.
- [6] Liu, Z. L., Deng, J. L., Deng, J. J., and Li, F. F. 2008. "Fabrication and Photocatalysis of CuO/ZnO Nano-composite via a New Method." *Materials Science and Engineering B* 150 (2): 99-104.
- [7] <https://www.researchgate.net/publication/321017142>. UV/VIS Spectrophotometry-Fundamentals and Applications.